

# Examining the effects of cooling/lubricating conditions on tool wear in milling Hastelloy X

**Christopher T. Tyler and Tony L. Schmitz**  
Mechanical Engineering and Engineering Sciences  
University of North Carolina at Charlotte  
Charlotte, NC

## ABSTRACT

High tool wear rates serve as a leading factor that limits the machinability of nickel-based alloys. The high strength and corrosion/creep-resistant properties that make these materials attractive to the designer also make them challenging to machine by causing increased cutting edge temperatures and decreased tool life. This paper details the wear mechanisms and tool life when milling Hastelloy X using both cryogenic CO<sub>2</sub> and minimum quantity lubrication (MQL) as cooling/lubricating solutions. Experiments were conducted using a physical vapor deposition (PVD) TiAlN coated carbide bull nose cutter. Cutting forces were used in conjunction with microscope and thermal images to compare the performance of the two approaches. Results showed that MQL methods produced a predictable mode of tool failure, while cryogenic cooling significantly reduced the tool life and resulted in catastrophic failure modes.

## KEYWORDS

Milling, wear, nickel-based alloys, cryogenic machining, MQL

## INTRODUCTION

Nickel-based super alloys serve as important materials in the aerospace, gas turbine, and nuclear industries. These alloys are highly regarded for superior corrosion, creep, and thermal fatigue resistance. In particular, Hastelloy X is widely used within the combustion regions of gas turbines where temperatures exceed 1100°C for several thousand hours [1]. It derives its unique mechanical properties from a high composition percentage of solid-solution elements including: Cr-22%, Fe-18%, Mo-19%, and Co-1.5%. The desired mechanical properties also contribute to its poor machinability. The characteristics of its machinability can be summarized as follows [2-6]:

- rapid work hardening during machining operations.
- abrasive tool wear due to carbides within the material
- poor thermal conductivity/diffusivity causes heat to remain at the cutting tool tip which yields high cutting edge temperatures
- diffusive wear due to high cutting edge temperatures and chemical interactions
- chip adhesion leads to notch wear and/or chipping along the cutting edge.

Oil emulsion and water-based cutting fluids are the conventional method for cooling/lubrication when cutting difficult-to-machine materials. However, the environmental and health concerns associated with the use of these fluids are driving the demand for alternative machining strategies. These strategies include, for example, dry machining using ceramic cutters, minimum quantity lubrication (MQL), chilled air, and cryogenic machining [7].

Among these methods, the use of cryogenic fluids is an attractive cooling alternative. It cools the cutting zone to very low temperatures using liquefied gases, such as liquid nitrogen (N<sub>2</sub>), helium (He), or carbon dioxide (CO<sub>2</sub>). Investigations involving cryogenic cooling are leading to advancements in tool performance and overall part quality. The influence of cryogenic nitrogen machining, for example, has notably improved the tool life, surface finish, and residual compressive stresses in the turning of magnesium alloys, NiTi-shape memory alloys, and titanium alloys [8-10].

CO<sub>2</sub> cooling has been shown to improve the tool life in polycrystalline diamond (PCD) turning of compacted graphite iron (CGI), but the performance is highly dependent on grain size and binder content of the tool material [11]. It has also been shown to also suppress burr formation and limit notch wear in the turning of  $\beta$ -titanium alloys by a factor of two over conventional emulsion flood coolant [12].

Predominately, cryogenic cooling has positively impacted the cutting performance of hard-to-machine materials during uninterrupted cutting operations. However, its effect on interrupted cutting operations, such as milling, is not well understood, although some studies are reported in the literature. For example, Su *et al.* observed improved tool life in the high speed milling of Ti-6Al-4V using compressed nitrogen gas, but also observed instances of dramatically reduced tool life due to thermal fatigue cracking of the tool [13]. Also, Supekar *et al.* describe an average flank wear suppression during milling of CGI over conventional emulsion flood coolant.

This paper examines the cutting performance of milling Hastelloy X using two cooling/lubricating strategies. The effects on tool life, cutting forces, and cutting temperatures are examined using an aqueous-based MQL coolant and cryogenic CO<sub>2</sub> spray.

**EXPERIMENT DESCRIPTION**

Machining investigations were conducted using a conventional three-axis CNC mill (Haas TM-1) with a maximum spindle speed of 4000 rpm and maximum spindle power output of 5.6 kW. A four-flute, solid-body, TiAlN (PVD) coated carbide cutter (Sandvik R216.24-10050EAK22P) was used. The bull nose cutter was 10 mm in diameter and had a nominal nose radius of 2 mm. Cutting forces, cutting temperatures, digital microscope images, and scanning electron microscope images were used to assess the tool performance under the two cooling/lubricating conditions.

**Measurement and Cutting Parameters**

The cutting forces were measured using a piezo-multicomponent dynamometer (Kistler 9257B); see Figure 1. This enabled dynamic measurement of the three orthogonal components of the cutting force during each milling operation. A 152 mm × 101 mm × 16 mm Hastelloy X workpiece was secured to the dynamometer and tests cuts were performed using the parameters presented in Table 1. All cutting tests were climb (down) milling operations.

**Table 1.** Cutting test parameters.

Cutting speed, $V$ (m/min)	44, 50, 71
Feed per tooth, $f_t$ (mm/tooth)	0.05
Axial depth of cut, $b$ (mm)	4.0
Radial depth of cut, $a_r$ (mm)	2.0
Length of cut, $l_c$ (mm)	101



**Figure 1.** Milling setup using a cutting force dynamometer.

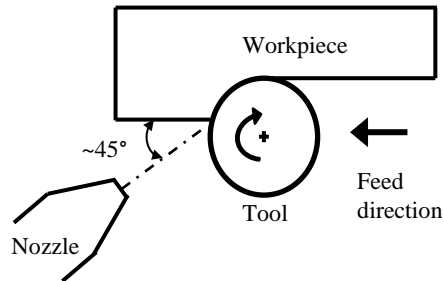


**Figure 2.** MQL/CO<sub>2</sub> nozzle position relative to workpiece and cutting tool.

To avoid removing the tool from the spindle, a portable digital microscope (Dyno-lite AM-413T) was used to record the flank wear width (FWW) at regular intervals. This enabled both qualitative and quantitative assessment of the cutting edges. The end of life criterion was defined to be a maximum FWW of 300 μm. Each FWW measurement was recorded as the average of the maximum wear on each cutting edge. Cutting temperatures were measured using a hand-held infrared camera (FLIR-i7) and used as a qualitative comparison between the two cooling/lubricating strategies.

**Cooling and Lubricating Conditions**

Two types of cooling/lubricating strategies were investigated in this study. The first was a water-based MQL mist coolant. The nozzle was inclined approximately 45° relative to the feed direction and directed at the entrance of the cut, where cutting force magnitudes are highest for climb milling; see Figure 2. The nozzle was positioned approximately 50 mm from the tool. The volumetric flow rate was measured to be approximately 20 ml/min.

The second was cryogenic CO<sub>2</sub> spray. The supply of CO<sub>2</sub> was controlled through a coaxial delivery assembly. Pressure-regulated propellant gas flowed through the outer delivery tube. In this case, clean, dry compressed air was supplied at a maximum pressure of 827 kPa. A solid particle CO<sub>2</sub> stream flowed through an inner capillary tube. The CO<sub>2</sub> was stored in a gas cylinder in liquid form and siphoned from the container using a dip tube (the CO<sub>2</sub> experiences a phase transformation from liquid to solid state via the Joule-Thompson throttle effect). A soy-based lubricant was mixed with the coolant and supplied at approximately 5 ml/min.

Two experiments were conducted to observe the effects of mass flow rate of CO<sub>2</sub> on the cutting performance. Initially, CO<sub>2</sub> was delivered at a mass flow rate of 6.8 kg/hr. In subsequent testing, the flow rate was adjusted to a manufacturer-recommended 5.4 kg/hr. The nozzle for all CO<sub>2</sub> experiments was positioned in approximately the same orientation as the MQL experiments; see Figure 2.

For the testing, the dynamometer was not exposed to extreme temperatures for excessive periods of time. The top plate of the dynamometer was factory coated with a thermal isolation coating [14], so there was little concern that the lower temperatures affected the cutting force measurements.

**RESULTS**

The intent of this study was to perform a one-to-one tool life comparison using the two methods. The tool life was recorded as the total cutting time to reach a maximum FWW of 300 μm. Table 2 presents a comparison of the total volume removed and tool life between the MQL and CO<sub>2</sub> strategies. The CO<sub>2</sub> mass flow rate was approximately 6.8 kg/hr, the maximum rate available.

**Table 2.** Tool life comparison between cooling strategies.

Cutting speed (m/s)	Spindle speed (rpm)	Volume removed (cm <sup>3</sup> )		Tool life (min)	
		MQL	CO <sub>2</sub>	MQL	CO <sub>2</sub>
44	1400	160	17.6	71.4	7.9
50	1600	70.4	19.2	27.8	7.5
71	2250	3.2	4.8	0.89	1.8

From the table, the MQL tool life tests follow a clear trend: as the cutting velocity was increased, the tool life decreased. In fact, a Taylor tool life model, which relates

the tool life, *T*, to the cutting speed using a power law, was constructed using the form [15]:

$$VT^n = C, \tag{1}$$

where *n* = 0.107 and *C* = 70.6 (R<sup>2</sup> = 0.98); see Figure 3.

The tool life in the CO<sub>2</sub> cutting experiments did not follow such a clear trend and was observed to be significantly lower than the MQL tests. The percent change in tool life was approximately -89% for the lowest cutting speed of 44 m/s.

At the suggestion of the cryogenic system manufacturer, the mass flow rate was adjusted to a lower nominal rate of 5.4 kg/hr. Cutting tests were repeated at the midrange speed of 50 m/s to see if there was any improvement in machining performance. The tool life was approximately 7.2 minutes for the new CO<sub>2</sub> parameters. This was similar to the tool life for the initial CO<sub>2</sub> test and still much lower than the MQL tool life.

Additional data was collected to provide further qualitative and quantitative comparisons between the two cooling strategies and draw possible conclusions for the contradictory results.

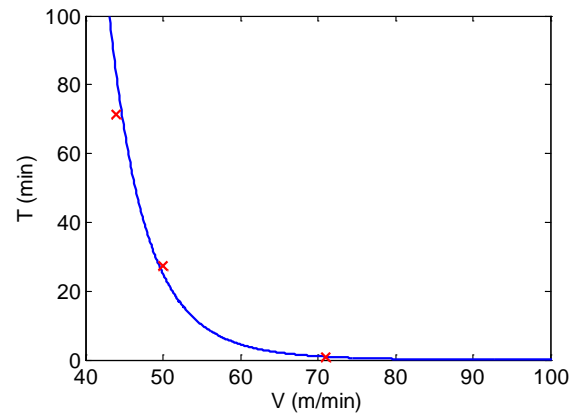


**Figure 3.** Tool life model fit for MQL cutting experiments.

**Digital Microscope Comparison**

Digital microscope images were captured at frequent intervals throughout each of the cutting trials. This enabled convenient assessment of the tool cutting edges, including the ability to measure the wear levels.

Figure 4 illustrates the wear progression in the 50 m/s MQL cutting trial. Figure 4a shows the condition of the cutting edge after approximately 13.8 minutes of cutting (44 passes). Figure 4b displays the cutting edge at the end of life (27.8 minutes, 89 passes). No observable edge chipping or other failure modes were observed in the microscope images.

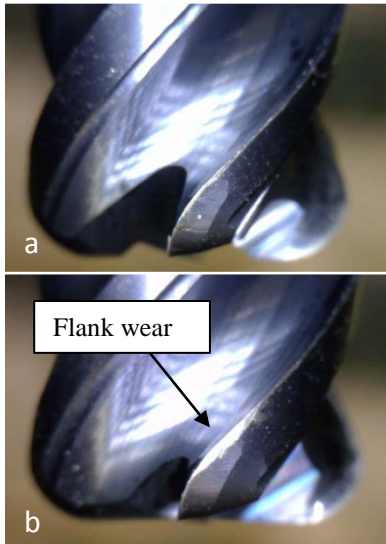


**Figure 4.** Flank wear progression during MQL tests at a cutting speed of 50 m/s: a) 13.8 minutes (44 passes); and b) 27.8 minutes (89 passes).

The failure mode observed during the CO<sub>2</sub> tests was different from the MQL tests. Cutting edge fracture was observed to occur early in the cutting tests. Figure 5a displays an example of edge chipping at 50 m/s after 6.3 minutes (20 passes). This led to catastrophic failure of the cutting tool after only four additional passes; see Figure 5b.

### SEM Comparison

The cutting edge was further assessed using a JEOL-6480 scanning electron microscope (SEM) for MQL and both CO<sub>2</sub> mass flow rates (6.8 kg/hr and 5.4 kg/hr). Figure 6 shows the cutting edge under MQL conditions after 7.8 minutes of use at the 50 m/s cutting speed. As observed in the digital microscope images, the edge is intact and a uniform level of wear is present along its length.

Figure 7 confirms the cutting edge chipping phenomenon for the 6.8 kg/hr CO<sub>2</sub> trials. The edge damage occurred after 3.8 minutes of cutting at the 50 m/s cutting speed and is consistent with the damage observed in the digital microscope images.

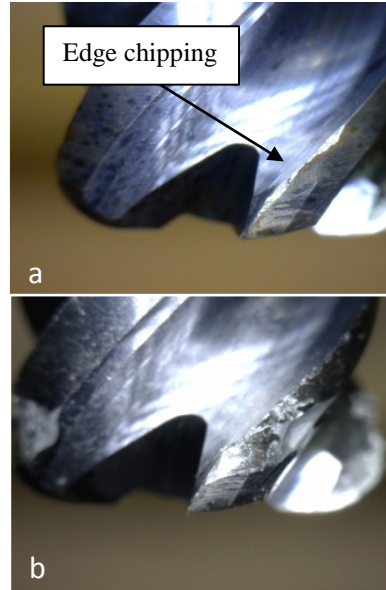


**Figure 5.** a) Chipping of the cutting edge during 50 m/s cutting tests after 6.3 minutes (20 passes). b) Catastrophic failure of tool after 7.5 minutes (24 passes).

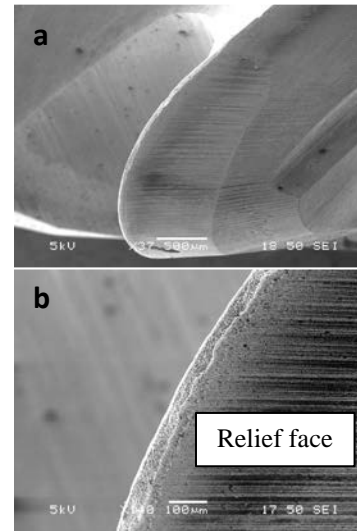


**Figure 6.** SEM image of cutting edge under MQL conditions at: a) 37x magnification; and b) 110x magnification

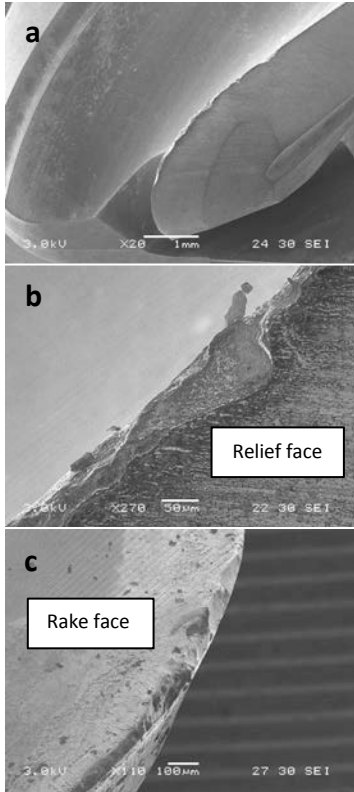


**Figure 7.** Edge chipping at: a) 20x; b) 270x; and c) 110x magnification under CO<sub>2</sub> cooling conditions after 3.8 minutes of cutting (6.8 kg/hr).

Similarly, as shown in Figure 8, edge chipping was also observed for the second CO<sub>2</sub> trial in which the mass flow rate was lowered to 5.4 kg/hr. The edge damage shown occurred after approximately 7.2 minutes of use. This is approximately the same amount of cutting time in which Figure 6 depicts the MQL wear state. It is also interesting to see in Figure 7a what appears to be a type of abrasive wear along present along the relief face of the tool that was not present under MQL conditions.

**Cutting Force Comparison**

It is anticipated that the onset of cutting edge fracture reduces the ability of the cutter to properly shear the material and, consequently, leads to increased cutting forces. Figure 9 compares total cutting forces between cooling strategies for the 50 m/s cutting speed. The cutting force magnitude was calculated as:

$$\|F\| = \sqrt{\bar{F}_x^2 + \bar{F}_y^2 + \bar{F}_z^2}, \quad (2)$$

where  $\bar{F}_i$  is the mean of the  $i$ -component force from five seconds of cutting.

Figure 9 illustrates the effect of continual edge chipping on the cutting force. There is a sharp increase in force with progressive cutting passes. Alternately, the force gradually increased with cutting time for the MQL tests. This is consistent with a uniformly increasing wear level.

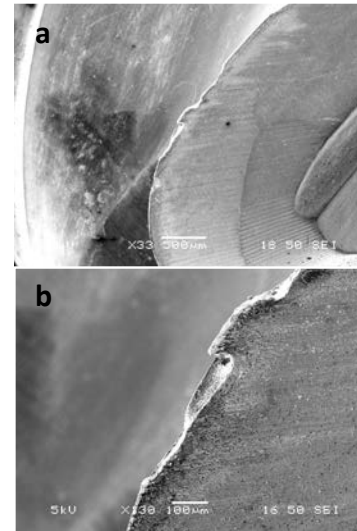


**Figure 8.** Edge chipping at: a) 33x; and b) 130x magnification under CO<sub>2</sub> cooling conditions after 7.2 minutes of cutting (5.4 kg/hr).

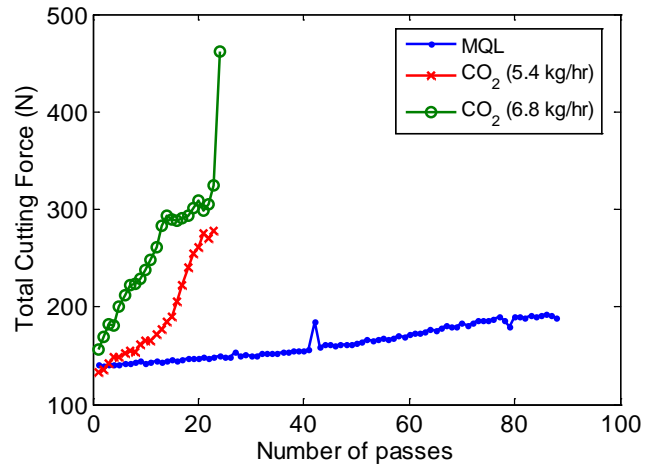


**Figure 9.** Influence of cooling strategy on total cutting force.

### Thermal Comparisons

Temperature was measured during the cutting processes using an infrared camera (Flir-i7). The emissivity of the workpiece's surface was assumed to be 0.21 for all thermal measurements. This is consistent with similar tests performed in turning of nickel-based alloys [9]. While it was not possible to precisely measure temperatures at the cutting edge during machining, it did enable the comparison of the effective cooling in the cutting region.

Figures 10 and 11 demonstrate the baseline temperatures observed in the CO<sub>2</sub> and MQL cooling, respectively, without any cutting being performed. The images were taken with the commanded spindle speed of 1600 rpm, which corresponded to the cutting speed of 50 m/s. Figure 10 shows a minimum temperature of approximately -4 °C with the mass flow rate of the CO<sub>2</sub> system set to 5.4 kg/hr. Figure 11 shows a cooling temperature of approximately 14 °C for the MQL strategy.

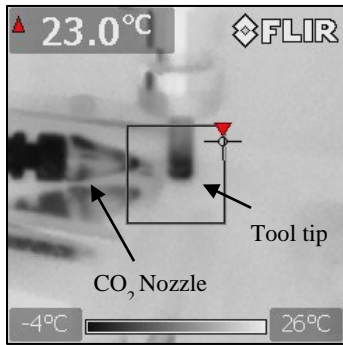


**Figure 10.** Baseline temperatures for CO<sub>2</sub> cooling at a mass flow rate of 5.4 kg/hr.

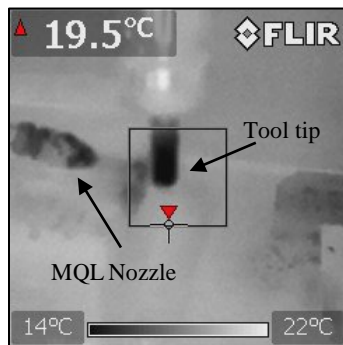


**Figure 11.** Baseline temperatures for MQL cooling.

The maximum cutting temperatures generated in the cutting region were similar for the two cooling strategies as shown in Figures 12-14. Figures 12 and 13 exhibit a

heated region that is localized to the effective cutting zone for the cryogenic cooling method with the 5.4 kg/hr and 6.8 kg/hr flow rates, respectively. As observed in Figure 14 for MQL, the heated zone radiates throughout the tool body and workpiece. The similar temperatures suggest that, although the CO<sub>2</sub> cooling method does cool the cutting edges while out of the cut, it cannot adequately cool the localized shearing zone where temperatures are highest.

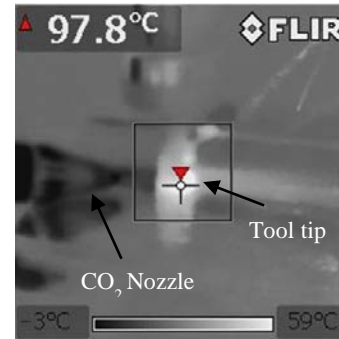


**Figure 12.** Cutting temperatures generated during machining with CO<sub>2</sub> cooling at 5.4 kg/hr and 50 m/s cutting speed.

### DISCUSSION

The results presented in this study depict an adverse impact on tool life when milling Hastelloy X using cryogenic CO<sub>2</sub> cooling compared to MQL. As revealed by digital microscope and scanning electron microscope images, there is an edge chipping phenomenon observed when using CO<sub>2</sub> to cool the cutting zone that does not occur under MQL conditions. The following paragraphs provide possible explanations for the diminished cutting performance.

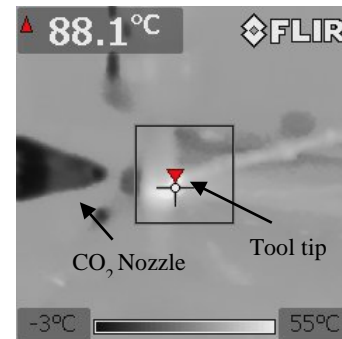


**Figure 13.** Cutting temperatures generated during machining with CO<sub>2</sub> cooling at 6.8 kg/hr and 50 m/s cutting speed.

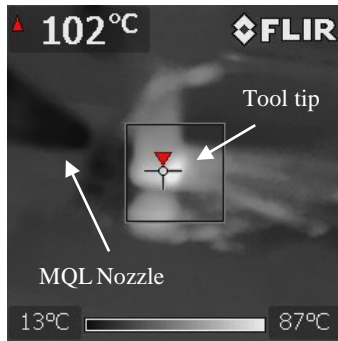


**Figure 14.** Cutting temperatures generated during machining with MQL cooling and 50 m/s cutting speed.

Many investigations into the influence of cryogenic cooling strategies on tool life have been performed for turning operations. In the case of turning, there is continuous heat generated at the primary cutting zone that cooling systems serve to minimize. However, for interrupted cutting during milling, there is a repeated cycling of extreme hot and cold working conditions. This could lead to a form of thermal fatigue which, in the case of high speed milling of Ti-6Al-4V [13, 16], has been observed to cause chipping and fracture of cutting tools and greatly reduce the tool life.

The reduction in cutting force (Figure 9) after reducing the amount of CO<sub>2</sub> being delivered to the tool edges supports the thermal cycling theory and subsequent edge fracture. Decreased cooling reduced the temperature variation of the tool between in-cut and out-of-cut conditions, which reduced the edge fracture due to fatigue.

Another plausible explanation for the rapid tool edge failure under cryogenic conditions is either built-up edge (BUE) or chip adhesion. Kadirgama *et al.* and Sharman *et al.* demonstrated that BUE or chip adhesion could strip the coating from the cutter in the turning of Inconel 718 and Hastelloy C-22HS [6,17]. The presence of BUE led to exposure of the tungsten carbide; jagged edges and a rapid degradation in tool life was observed. This could explain the cause for chipping in the case for milling. However, there was no evidence of adhesion found in the microscope images. Similarly, the temperature of CO<sub>2</sub> spray may have caused the tool's TiAlN coating to become brittle and chip when encountering the high cutting forces. Finally, the excessive cooling has been shown to have an effect on the specific cutting energy in machining operations [18]. An increase in cutting stiffness of the cooled workpiece could also contribute to the accelerated tool failure during CO<sub>2</sub> machining.

## CONCLUSIONS

Excessive tool-wear proves to be one of the key obstacles when machining nickel-based superalloys. Due to the difficulties in machining these materials, various methods for cooling/lubrication are emerging. This study presented a comparison of tool life when using minimum quantity lubrication and cryogenic CO<sub>2</sub> as cooling/lubricating strategies in the milling of Hastelloy X.

Digital microscope images, SEM images, cutting force data, and thermal images were used compare the effectiveness of the two cooling methods. Results showed an approximate 89% longer tool life when using MQL compared to CO<sub>2</sub> for the selected cutting conditions. From microscope images, a clear edge chipping phenomenon occurred when using CO<sub>2</sub>. This led to larger cutting forces and, ultimately, sudden catastrophic failure of the tool edge.

Possible explanations for the adverse cutting performance using CO<sub>2</sub> include thermal fatigue cycling, material adhesion to the cutting edge, coating failure, and changes in workpiece material properties. The periodic large variations in temperature for the in-cut and out-of-cut times are proposed to have caused brittle cracking of the cutting edge in this study.

## ACKNOWLEDGEMENTS

The authors would like to express their gratitude to Siemens Energy for their partial support of this project.

## REFERENCES

- [1] Haynes Hastelloy Standard Product Catalogue, Haynes International, Indiana, 2007, pp. 2-7
- [2] Ezugwu, E.O., Z.M. Wang, and A.R. Machado. "The machinability of nickel-based alloys: a review." *Journal of Materials Processing Technology* 86.1 (1998): 1-16.
- [3] Richards, N., and D. Aspinwall. "Use of ceramic tools for machining nickel based alloys." *International Journal of Machine Tools and Manufacture* 29.4 (1989): 575-588.
- [4] Ezugwu, E. O., Z. M. Wang, and C. I. Okeke. "Tool life and surface integrity when machining Inconel 718 with PVD-and CVD-coated tools." *Tribology transactions* 42.2 (1999): 353-360.
- [5] Khidhir, B.A., and B. Mohamed. "Study of cutting speed on surface roughness and chip formation when machining nickel-based alloy." *Journal of mechanical science and technology* 24.5 (2010): 1053-1059.

- [6] Kadirgama, K., *et al.* "Tool life and wear mechanism when machining Hastelloy C-22HS." *Wear* 270.3 (2011): 258-268.
- [7] Shokrani, A., V. Dhokia, and S.T. Newman. "Environmentally conscious machining of difficult-to-machine materials with regard to cutting fluids." *International Journal of Machine Tools and Manufacture* 57 (2012): 83-101.
- [8] Pu, Z., *et al.* "Enhanced surface integrity of AZ31B Mg alloy by cryogenic machining towards improved functional performance of machined components." *International Journal of Machine Tools and Manufacture* 56 (2012): 17-27.
- [9] Kaynak, Y., *et al.* "Tool-wear analysis in cryogenic machining of NiTi shape memory alloys: A comparison of tool-wear performance with dry and MQL machining." *Wear* 306 (2013): 51-63.
- [10] Wang, Z.Y., and K.P. Rajurkar. "Cryogenic machining of hard-to-cut materials." *Wear* 239.2 (2000): 168-175.
- [11] Abele, E., and B. Schramm. "Using PCD for machining CGI with a CO<sub>2</sub> coolant system." *Production Engineering* 2.2 (2008): 165-169.
- [12] Machai, C., and D. Biermann. "Machining of  $\beta$ -titanium-alloy Ti-10V-2Fe-3Al under cryogenic conditions: Cooling with carbon dioxide snow." *Journal of Materials Processing Technology* 211.6 (2011): 1175-1183.
- [13] Su, Y., *et al.* "An experimental investigation of effects of cooling/lubrication conditions on tool wear in high-speed end milling of Ti-6Al-4V." *Wear* 261.7 (2006): 760-766.
- [14] Kistler Group, "Multicomponent Dynamometer -5 - 10 kN, Top Plate 100x170 mm," 9257B datasheet (2009).
- [15] Taylor, F.W. "On the art of cutting metals." *Transactions of the ASME*, Vol. 28 (1907): 31-248.
- [16] Uehara, K. "Fundamental approach to the thermal crack of cermet cutting tools." *CIRP Annals-Manufacturing Technology* 30.1 (1981): 47-51.
- [17] Sharman, A., R.C. Dewes, and D.K. Aspinwall. "Tool life when high speed ball nose end milling Inconel 718™." *Journal of Materials Processing Technology* 118.1 (2001): 29-35.
- [18] Pušavec, F., *et al.* "The influence of cryogenic cooling on process stability in turning operations." *CIRP Annals-Manufacturing Technology* 60.1 (2011): 101-104.